

Supplementary Information for

IFI16-dependent STING signaling is a crucial regulator of anti-HER2 immune response in breast cancer.

Li-Teng Ong¹, Wee Chyan Lee¹, Shijun Ma¹, Gokce Oguz¹, Zhitong Niu², Yi Bao¹, Mubaraka Yusuf¹, Puay Leng Lee¹, Jian Yuan Goh¹, Panpan Wang³, Kylie Su Mei Yong⁴, Qingfeng Chen⁴, Wenyu Wang², Adaikalavan Ramasamy¹, Dave SB Hoon⁵, Henrik J Ditzel^{6,7}, Ern Yu Tan⁸, Soo Chin Lee^{9,10}, and Qiang Yu^{1,11,12,*}

¹Genome Institute of Singapore, Agency for Science, Technology, and Research (A*STAR), Biopolis, Singapore

²The Sixth Affiliated Hospital of Sun Yat-sen University, Guangzhou, China

³Jinan University First Affiliated Hospital, Guangzhou, China

⁴Institute of Molecular and Cell Biology, Agency for Science, Technology and Research (A*STAR), Singapore

⁵Department of Translational Molecular Medicine, Saint John's Cancer Institute, Providence Health System, Santa Monica, CA, USA

⁶Department of Oncology, Odense University Hospital, Odense, Denmark

⁷Department of Cancer and Inflammation Research, Institute of Molecular Medicine, University of Southern Denmark, Odense, Denmark

⁸Department of General Surgery, Tan Tock Seng Hospital, Singapore

⁹Cancer Science Institute of Singapore, Yong Loo Lin School of Medicine, National University of Singapore, Singapore

¹⁰Department of Haematology-Oncology, National University Cancer Institute, National University Health System, Singapore

¹¹Department of Physiology, Yong Loo Lin School of Medicine, National University of Singapore, Singapore

¹²Cancer and Stem Cell Biology, Duke-NUS Medical School, Singapore.

*Correspondence should be addressed to Qiang Yu (yuq@gis.a-star.edu.sg)

This PDF file includes:

Methods and material

Figures S1 to S12

Tables S1 to S5

SI References

Methods and materials

Human samples

All human biological samples were collected with informed consent. The study was approved by the Ethics Committee of Tan Tock Seng Hospital (Singapore), the Ethics Committee of the Region of Southern Denmark (Denmark) and the Ethics Committee of Saint John's Cancer Institute (USA).

Cell lines and cell culture

All cell lines were obtained and cultured according to American Type Culture Collection (ATCC) instructions, unless otherwise stated. All cell lines used for functional studies were determined to be free of mycoplasma contamination. SKBR3, MDA-MB-231, MCF7, T-47D, MDA-MB-415, MDA-MB-361, BT-474, MDA-MB-468, BT-549, MDA-MB-157, Hs578T and MDA-MB-436 breast cancer cell lines, and Platinum-A cell (Plat-A) and HEK293T cell were cultured in DMEM (Hyclone; Cat. No. SH30243.FS), supplemented with 10% heat-inactivated FBS (Biowest; Cat. No. S1818BH). Plat-A cell line (Cat. No. RV-102) was obtained from Cell Biolabs (San Diego, CA). HCC1806, HCC1937, 4T1 and 4T1-HER2 breast cancer cell lines were maintained in RPMI (Thermo Fisher Scientific; Cat. No. A1049101) supplemented with 10% heat-inactivated FBS. The MCF10A normal breast epithelial cell line was cultured in DMEM/F12 (Invitrogen; Cat. No. 11330-032) supplemented with 5% horse serum (Invitrogen; Cat. No. 16050-122), 10 ng/mL EGF (Peprotech; Cat. No. AF-100-15), 0.5 mg/mL hydrocortisone (Sigma-Aldrich; Cat. No. H-0888), 100 ng/mL cholera toxin (Sigma-Aldrich; Cat. No. C-8052) and 10 µg/mL insulin (Sigma-Aldrich; Cat. No. I-1882). All culture media were supplemented with 100 U/mL penicillin-streptomycin (Thermo Fisher Scientific; Cat. No. 15140-122). All cell lines were maintained at 37°C in a humidified atmosphere at 5% CO₂.

Primary cells culture and stimulation

Human peripheral blood mononuclear cells (PBMCs) were isolated from peripheral blood by Ficoll gradient centrifugation (GE Healthcare; Cat. No. 17144002) and subjected to red blood cells lysis using RBC Lysis Buffer (Thermo Fisher Scientific; Cat. No. 00-4333-57). Human leukocyte antigen HLA-A2+ was identified by flow cytometry analysis. NK cells were expanded by culturing PBMCs in NK Cell Activation/Expansion Kit (Miltenyi Biotech; Cat. No. 130-094-483) containing CD335/CD2 antibodies in NK MACS medium (Miltenyi Biotech; Cat. No. 130-114-429) containing 5% human AB serum (Invitrogen; Cat. No. H4522) and 200 IU/uL rh-IL2 (Miltenyi Biotec; Cat. No. 130-097-748) for 1 week, followed by NK cell purification using an NK cell isolation kit (Miltenyi Biotech; Cat. No. 130-092-657). T cells were activated and expanded from PBMCs using TransAct medium (Miltenyi Biotech; Cat. No. 130-111-160) containing CD3/CD28 antibodies for 3 days prior

to T cell isolation using a pan-T cell isolation kit (Miltenyi Biotec; Cat. No. 130-096-535). T cells were maintained in TexMACS medium (Miltenyi Biotec; Cat. No. 130-097-196) containing 200 IU/uL rh-IL2 for 2 weeks before DC antigen stimulation. The purity of both immune cells were validated by flow cytometry. All mouse immune cells were cultured in RPMI1640 supplemented with 10% FBS containing 200 IU/uL rh-IL2. Mouse splenocytes were isolated from spleens of 4T1 or 4T1-HER2 tumor-bearing Balb/C mice. Briefly, 4T1 or 4T1-HER2 cells (5 x 10⁴ cells) were injected into the mammary fat pad of 8- to 12-week-old female Balb/C and spleens were collected when the tumor size reached ~100mm³ and pressed through sterile mesh filters using 5mL of RPMI medium to wash the screens. Splenocytes were then isolated by Ficoll gradient centrifugation. Mouse NK cells were negatively selected from splenocytes using CD49b (DX5) microbeads (Miltenyi Biotec; Cat. No. 130-052-501). T cells were negatively isolated using CD90.2 microbeads (Miltenyi Biotec; Cat. No.: 130-121-278).

Immune cell stimulation and activation

Activated human NK cells were obtained by subjecting NK cells to 10 ng/mL rh-IL12 (Biolegend; Cat. No. 573002), 5 ng/mL rh-IL15 (Biolegend; Cat. No. 570302) and 10 ng/mL rh-IL18 (Biolegend, San Francisco, CA; Cat. No. 592102) for 24 hours. To activate mouse cells, rm-IL12 (Biolegend; Cat. No. 577004), rm-IL15 (Biolegend; Cat. No. 566302) and rm-IL18 (Biolegend; Cat. No. 767004) were used. To generate antigen-specific human T cells, DC was first differentiated from HLA-A2+ PBMCs through stimulation of 20 ng/mL human IL4 (Miltenyi Biotec; Cat. No. 130-093-921) and 20 ng/mL human GM-CSF (Miltenyi Biotec; Cat. No. 130-093-864) in RPMI 1640 media containing 10 % FBS containing 200 IU/mL rh-IL2 for 7 days. Differentiated DC were then subjected to 100 ng/mL mHSP65 protein (Sigma-Aldrich; Cat. No. 16561-29-8) and 50 ug/mL cancer cell lysate (CCL) for further DC maturation and activation. After 3 days of CCL priming, DC was ready to be used for T cell stimulation. CCL was prepared by 6 snap-freeze-and-thaw cycles of SKBR3 or MDA-MB-231 cell suspension in PBS. For mouse T cell activation, 100 ng/mL PMA (Sigma-Aldrich; Cat. No. 16561-29-8) and 1 µg/mL ionmycin (Sigma-Aldrich; Cat. No. I9657) was added to mouse T cells for 24 hours before the experiment.

shRNA and siRNA transfections

All stable over-expressed cell lines were generated via retroviral infection using PlatA cells to package retrovirus, while all stable knockdown cell lines were transduced by the lentiviral method via viral packaging of HEK293T cells, unless stated otherwise. To generate breast cancer cell lines stably expressing luciferase, cells were infected with lentivirus packaged with pLenti-V5-luc (Addgene; Cat. No. 21474) for 24 hours, followed by blasticidin selection. For 4T1-HER2-luc cells, full length human cDNA of human HER2 gene was subcloned into PMN retroviral expression vector. Virally-infected cells were sorted based on GFP overexpression. To generate knockdown

cell lines, shRNA oligonucleotides were subcloned into pLKO.1-puro (Addgene; Cat. No. 8453) vector according to the protocol available on Addgene (<http://www.addgene.org/tools/protocols/plko/>). An empty vector was included as a negative control. In brief, HEK293T cells were transfected with 4.5 µg of shRNA plasmid construct together with 1.5 µg of pMD2.G (Addgene; Cat. No. 12259), 1.5 µg of pMDLg/pRRE (Addgene; Cat. No. 12251) and 1.5 µg of pRSV-Rev (Addgene; Cat. No. 12253) using Lipofectamine 2000 (Invitrogen; Cat. No. 1168.019). Cells were transduced with lentivirus supernatant for 18 hours in the presence of 8 µg/mL polybrene. Cells were selected and maintained in puromycin. The shRNA oligonucleotides used for cloning are listed in supplementary table 3.

All siRNA transfections were conducted using dicer siRNAs (DsiRNAs) predesigned by Integrated DNA Technologies (IDT; Singapore) and transfected using Lipofectamin RNAiMax (Invitrogen; Cat. No. 13778-150) following the manufacturer's instruction. Predesigned non-targeting DsiRNAs, siNC (IDT; Cat. No. 51-01-14-03) was used as the negative control. The specific targeted sequences are listed in supplementary table 4.

Cell lysis assay

Breast cancer cells stably expressing luciferase were cocultured with immune cells for 48 hours before measuring luciferase activity by adding 1x luciferase substrate luciferin (Promega; Cat. No. P1043). Chemiluminescent signals were detected by GlowMAX Explorer (Promega) and the measurement was used to indicate cell viability against cells without coculture treated with the same concentration of relevant epigenetic drugs or combinations. Percent cell lysis was calculated using the formula below:

$$\% \text{ cytotoxicity} = 100 - \left(\frac{\text{Luciferase measurement of cocultured samples}}{\text{Luciferase measurement of noncocultured samples}} \right) \times 100 \%$$

Protein extraction and immunoblotting

Cells were lysed on ice in RIPA buffer containing protease and phosphatase inhibitors and further sonicated using XL2000 Microson Ultrasonic Processor (Misonix). Total protein concentration was determined using the Bradford reagent (Biorad, Cat. No. S000006). Proteins were resolved by SDS-PAGE under reducing conditions and electrotransferred onto polyvinylidene difluoride (PVDF) membrane (Sigma-Aldrich; Cat. No. IPVH00010). Membranes were then blocked with TBST blocking buffer containing 5% non-fat milk or BSA, followed by probing with the following antibodies: IFI16 (Santa Cruz; Cat. No. sc8023; 1:500), IFI204 (Thermo Fisher Scientific; Cat. No. PA5-23494; 1:500), phos-TBK1 (Cell Signalling Technology; Cat. No. 5483s; 1:1000), TBK1 (Cell Signalling Technology; Cat. No. 38066s; 1:1000), phos-IRF3 (Cell Signalling Technology; Cat. No. 37829s; 1:1000), phos-IRF3 (Cell Signalling Technology; Cat. No. 4947s; 1:1000), IRF3 (Cell Signalling Technology; Cat. No. 4302s; 1:1000), STING (Cell Signalling Technology; Cat. No. 13647s;

1:1000), H3k27me3 (Upstate Biotechnology; Cat. No. 07-449; 1:1000), H3k27ac (Upstate Biotechnology; Cat. No. 06-599; 1:1000), H3 (Cell Signalling Technology; Cat. No. 9715s; 1:1000), HER2 (Cell Signalling Technology; Cat. No. 2248s; 1:1000), EZH2 (Cell Signalling Technology; Cat. No. 5246; 1:1000), GAPDH (Cell Signalling Technology; Cat. No. 2118s; 1:2000), actin (Sigma-Aldrich; A2228; 1:4000) and tubulin (Cell Signalling Technology; Cat. No. 2128). Protein bands were detected by enhanced chemiluminescence on ChemiDoc Touch Gel and Western blot Imaging System (Bio-Rad Laboratories). All full blots are provided in the Supplementary file.

Quantitative RT-PCR analyses

Total RNA from cells or fresh frozen tumor samples was extracted using a Direct-zol™ RNA MiniPrep kit (ZymoResearch; Cat. No. R2052) as described by the manufacturer. For fresh-frozen tumors, samples were first homogenized with Qiagen TissueLyzer II (Hilden, Germany) before RNA extraction. Reverse transcription and Quantitative RT-PCR (qRT-PCR) reactions were performed using a High Capacity cDNA Reverse Transcription Kit (Applied Biosystems; Cat. No. 4368814) on a T100 Thermal Cycler (Bio-Rad), and KAPA SYBR FAST qPCR kit (Roche Holding AG; Cat. No. KK4620) on ViiA7 Real-Time PCR System (Thermo Fisher Scientific) in a 96- or 386-well plate formats. GAPDH level was used as an internal control for normalization. qRT-PCR primer sequences are listed in supplementary table 2.

RNA sequencing

Fresh-frozen tumors were obtained from Odense University Hospital, Denmark. Approximately 1µg of total RNA was extracted from each of the 13 primary human breast tumors and 7 metastatic breast tumors. RNA-seq libraries for the Illumina platform were generated and sequenced at NovogeneAIT (Singapore). Briefly, the mRNA were enriched using oligo(dT) beads and randomly fragmented to be used as templates to synthesize cDNA with random hexamers primers. The second-strand synthesis was then performed by incorporating oligonucleotides. Fragmentation and adaptor introduction were performed to obtain 250 – 300 bp. A full-length double-stranded cDNA library was completed through size selection and PCR enrichment. A pooled multiplexed library was sequenced on an Illumina sequencer.

For data processing and analyses, paired-end sequenced reads were first examined for quality control (FastQC v0.11.9 (1) and MultiQC v1.10 (2)) before alignment to human genome hg38 reference (HISAT2 v2.2.1 (3)) to generate read counts (featureCounts v2.0.2 (4)). Quality control for various alignment metrics was done with RSeQC (5). The raw count data was then normalized and rescaled to counts per 1 million (CPM). All downstream analyses were performed using R statistical programming. Differentially Expressed Gene between primary tumors and metastatic samples were defined using the edgeR(v3.32.1) package (6, 7) where genes showing $|\text{LogFC}| > 1$

in expression and adjusted p-value <0.05 (the cutoff value) were considered as significantly differentially expressed. Interferon Stimulated Genes (ISGs) were selected from Interferome database (8). 630 genes that appeared more than 3 times in the 142 database of randomly selected 51 individual experiments were selected as ISGs. Antigen-related gene set “KEGG_ANTIGEN_PROCESSING_AND_PRESENTATION” was downloaded from MsigDB (9, 10). Pre-ranked GSEA analysis was performed using clusterProfiler (v.3.18.1) (11) against MSigDb-Hallmark Datasets (9, 10).

To analyze the involvement of immune cells in solid tumors, Immune Cell Gene Signature (ImSig) (12) was performed using R programming. To calculate the relative abundance of immune cells across samples, Transcripts Per Million (TPM) normalized expression data was used with a correlation threshold set to 0.6. To quantify relative fractions of distinct cell types within samples, CIBERSORTx (13) was performed using well-established LM22 signature. Immune cell types that are present (infiltration >0%) in more than 75% of tumors were included for correlation analysis. Spearman’s correlation was used to calculate the correlation between gene expression of EZH2/HDAC1-3 and cell fractions deconvoluted by CIBERSORTx and, the expression of IFI16 across samples.

Microarray analysis

Two sets of microarray analyses were performed. The first microarray array set consisted of RNA extracted from basal (HCC1806, BT-549, MDA-MB-157, HS578T, MDA-MB-436, HCC1937 and MD-MB-231) and luminal (MCF7, T-47D, SKBR3, MDA-MB-415, MDA-MB-361, BT-474 and MDA-MB-468) breast cancer cell lines to identify their IRG gene expressions. The second set consisted of two epigenetic drug combination-treated SKBR3 (DZNep and TSA, D9 and ENT, and EPZ and ENT). RNA extracted from these cells was used for expression microarray analysis with the Illumina Gene Expression Sentrix BeadChip HumanHT-12_V4 (Illumina) and data analysis was performed using GeneSpring GX software (Agilent Technologies). The differential expression gene sets (fold change ≥ 1.6) were then subjected to Ingenuity Pathway Analysis (IPA) to identify the gene expression comparison of basal versus luminal breast cancer cell lines, and D9- and ENT- versus EPZ- and ENT-treated SKBR3 cells.

Breast cancer survival analyses of a public data set

Survival analyses for relapse-free survival (RFS), distant metastasis-free survival (DMFS) and overall survival (OS) were performed using the online database Gene expression-based Outcome for Breast cancer Online (GOBO) analysis (<http://co.bmc.lu.se/gobo/>). 3 quantiles for 10 years were selected to generate survival curves. The ER status of each subject was derived from the gene expression data set. All other parameters were left at default settings unless otherwise stated.

Chromatin Immunoprecipitation (ChIP) Assay

ChIP assays were performed as described previously with minor modifications. Briefly, 5 million cells (per sample) were cross-linked in 1% formaldehyde in culture medium for 10 min and the reaction was halted by the addition of 0.125 M glycine for 10 min at room temperature. Cell pellets were washed with ice-cold PBS twice and lysed in SDS lysis buffer (50mM Tris-HCl pH8.0, 10 mM EDTA, 1% SDS) for 5 min on ice, followed by sonication using Branson Digital Sonifier (Emerson) to obtain sheared chromatin. Soluble chromatin was then pre-cleared with Protein G Agarose (Roche; Cat. No. 05015952001) pre-coated with anti-rabbit IgG antibody (Santa Cruz; Cat. No. sc2027) in dilution buffer (10mM Tris-HCl pH7.4, 140 mM NaCl, 1 mM EDTA, 1 % Triton X-100, 0.01% SDS). Pre-cleared chromatin was then immunoprecipitated in anti-EZH2 (Active Motif; Cat. No. 39901), anti-H3K27me3 (Cell Signaling Technologies; Cat. No. 9733), anti-H3K27ac (Abcam; Cat. No. ab3729) (50 mM Tris-HCl pH7.5, 10mM EDTA, 1% SDS) or control rabbit IgG overnight at 4°C. The antibody-chromatin complex was then captured using Dynabeads (Invitrogen; Cat. No. 10004D) at 4 °C for 2 hours, followed by elution and reverse crosslinking in TE buffer (50mM Tris-HCl pH7.5, 10mM EDTA, 1% SDS) at 68°C overnight. Enzymatic digestion was performed using 20 mg/mL of Proteinase K at 42 °C for 2 hours, and the DNA was subsequently cleaned up using a QIAquick PCR Purification Kit (Qiagen; Cat. No. 28104). The immunoprecipitated and input DNA were quantified by qRT-PCR analysis using the primers listed below. Quantification of promoter-binding enrichment was calculated by normalizing the specific antibody against the input DNA. Data was presented as fold change relative to actin promoter. Primers used were listed in supplementary table 5.

For ChIP-seq analysis, precipitated chromatin DNA was sent to Novogene (China) for library preparation and sequenced in HiSeq2500 (Illumina). ChIP-seq data were aligned to reference genome hg38 by Bowtie2 v2.4.1 (14). SAMtools v1.7 (15) and Picard v2.23.3 (<http://broadinstitute.github.io/picard>) were used to detect and remove the aligned reads that are marked as duplicates, mapping to the blacklisted regions and/or multiple locations and/or different chromosomes. Normalized bigwigs were generated via bamCoverage command from deepTools(v3.4.3) (16). H3K27Ac and H3K27me3 peaks were identified using MACS2 (17) using input sequences as a background control. Peaks were annotated to the nearest gene features using ChIPseeker (18). Genes with H3K27me3^{hi/low} and H3K27ac^{low/hi} were selected as unique genes that appeared in each annotated gene list. These gene lists were subsequently intersected with the 104 IRG for peak annotation and enrichment parameters. For genes with multiple annotated peaks, peaks were merged for analysis. Genes were sorted by their fold enrichment value.

Flow cytometry analysis

For mouse *ex vivo* analysis, tumors or splenocytes were finely chopped using a scalpel and dissociated in a mouse tumor dissociation kit (Miltenyi Biotec; Cat. No. 130-096-730) according to manufacturer's protocol. The samples were passed through a 0.45 µm filter to obtain single-cell suspensions and washed twice in PBS. For splenocyte samples, lymphocytes were collected using Ficoll gradient centrifugation. For tumor samples, dissociated cells were incubated with 1x Live/Dead Fixable Dead Cell dye (Invitrogen) in ice-cold PBS for 20min to exclude dead cells from analysis. All *ex vivo* samples were stained with anti-mouse Fc γ R antibody (Miltenyi Biotec; Cat. No. 130-092-575) on ice for 20 min. For human cancer cell lines or immune cell analysis, cells were prestained with anti-human Fc γ R antibody (Miltenyi Biotec; Cat. No. 130-059-901). After Fc γ R antibody staining, cells were washed and stained for fluochrome-conjugated antibodies for specific surface markers for 30 min, followed by fixation using 1% formaldehyde in PBS. All flow cytometry analysis was carried out using MACSQuant (Miltenyi Biotec) or BD LSR II flow cytometer (BD Bioscience). Data were analyzed using FlowJo software (BD Bioscience).

The following antibodies were used. For mouse tumor analysis: anti-mouse CD45 PerCP-Cy5.5 (Biolegend; Cat. No. 103132), anti-mouse CD3 BV421 (BD Biosciences; Cat. No. 564008), anti-mouse CD4 BV650 (BD Biosciences; Cat. No. 563747) anti-mouse CD8 APC-Cy7 (Miltenyi Biotec; Cat. No. 130-120-737) and anti-mouse CD335 APC (Miltenyi Biotec; Cat. No. 130-112-202). For mouse memory T cells population: anti-mouse CD4 PE (BD Biosciences; Cat. No. 553048), anti-mouse CD8 APC-Cy7 (Miltenyi Biotec; Cat. No. 130-120-737), anti-mouse CD3 BV421 (BD Biosciences; Cat. No. 564008), anti-mouse CD45 FITC (Biolegend; Cat. No.103108), anti-mouse CD44 BV785 (Biolegend; Cat. No.103059) and anti-mouse CD62L BV711 (Biolegend; Cat. No. 104445). For human cancer cells' MHC expression: anti-human HLA-ABC FITC (Miltenyi Biotec; Cat. No. 130-120-432) and anti-human HLA-DR/DP/DQ FITC (Miltenyi Biotec; Cat. No. 130-123-938). For human memory T cells population: anti-human CD4 PE (Biolegend; Cat. No. 357404), anti-human CD8 FITC (Miltenyi Biotec; Cat. No. 130-110-671), anti-human CD62L BV650 (Biolegend; Cat. No. 304832) and anti-human CD45RO (Biolegend; Cat. No. 304234).

Statistical analysis

The sample size was based on the number of samples available for analysis. Animals were only excluded if they died or had to be sacrificed according to our IACUC protocol. No statistical method was used to predetermine sample size. Experiments and data analysis were not performed blinded to the conditions of the experiments. All *in vitro* experiments were performed at least twice at technical triplicates unless stated otherwise. For *in vivo* experiments, animals were randomized and treated as indicated in the experiments. All statistical analyses were performed with GraphPad Prism version 8.0, and are indicated in the figure legends. All data were presented as means \pm

SEM. Unless stated otherwise, statistical significance for assays was assessed using either one- or two-way analysis of variance (ANOVA) or Mann-Whitney unpaired t-test. All P values were two-sided, and significance was accepted at $P < 0.05$ unless otherwise stated: n.s., not significant, * $P \leq 0.05$, ** $P \leq 0.01$, *** $P \leq 0.001$ and **** $P \leq 0.0001$.

Data availability

RNA-sequencing data for primary and metastatic HER2+ breast tumors in Figure 1A was deposited at the NCBI Gene Expression Omnibus under accession code number [GSE191230](https://www.ncbi.nlm.nih.gov/geo/query/acc.cgi?acc=GSE191230). Uncropped Western blots, along with molecular weight standards, are included in supplementary data.

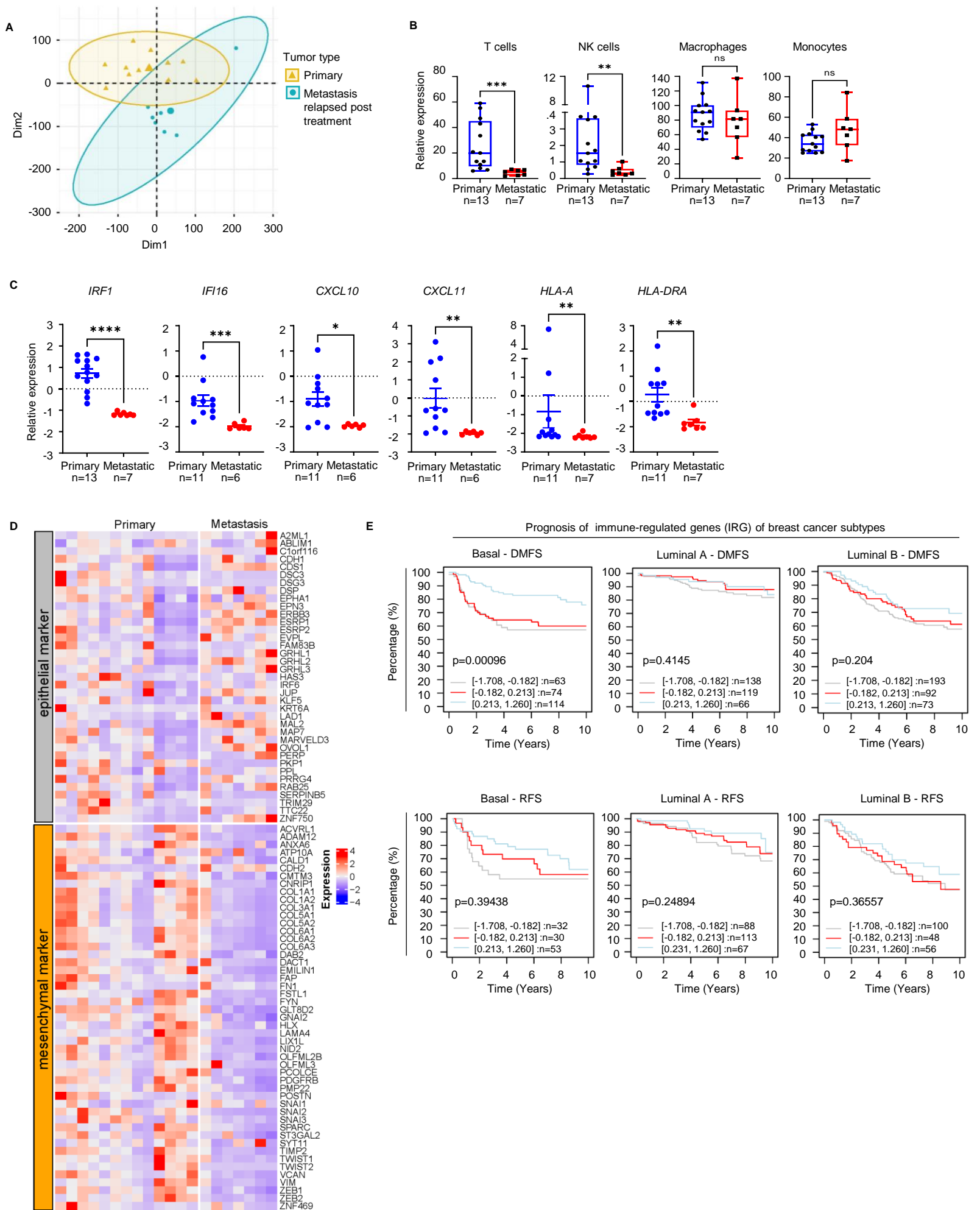
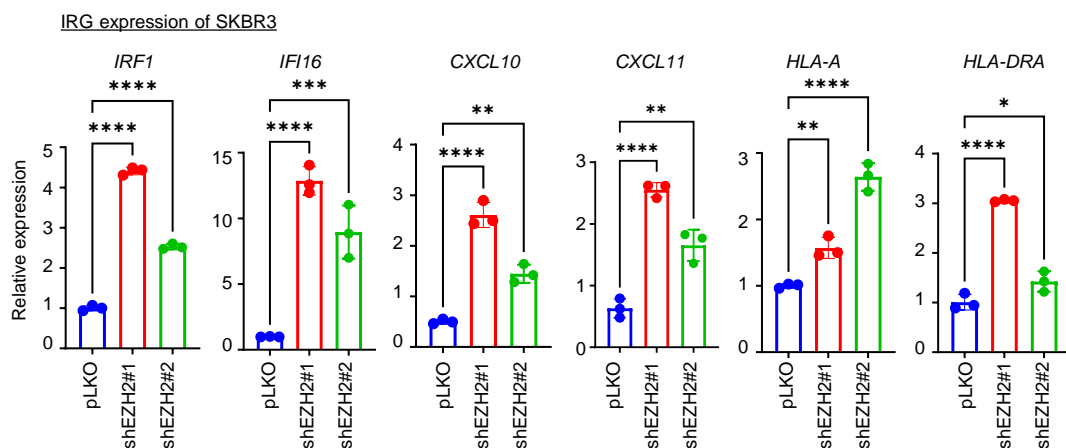
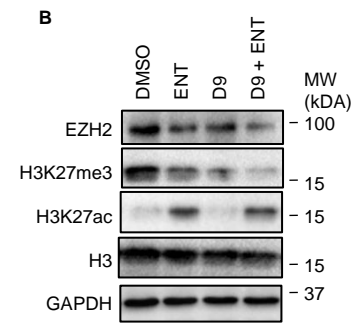


Figure S1: Downregulation IRG and IFN γ -secreting immune cells deliberates disease progression and poor anti-HER2 response in HER2+ breast cancer patients. (A) Principal component analysis showing differential gene expression of RNA-seq analysis separate most metastasis tumors ($n=7$) from primary tumors ($n=13$). **(B)** Immune Cell Gene Signatures for Profiling the Microenvironment of Solid Tumors (Imsig) of RNA-seq data showing T and NK cells are reduced in metastatic samples compared to primary HER2+ tumors. Other immune cells, including monocytes and macrophages, were not affected. **(C)** Representative IRG showing the downregulation in metastasis versus primary tumors as validated by RT-PCR. The data is presented in Z-score of fold change of gene expression relative to GAPDH. The number of subjects (n) per group is indicated in the graph. P values were calculated with Mann-Whitney unpaired t-test, * $P < 0.05$, ** $P < 0.01$, *** $P < 0.001$, **** $P < 0.0001$, ns not significant. **(D)** Heatmap showing EMT genes expression of RNA-seq samples **(E)** Kaplan-Meier plots showing distant metastasis-free survival (DMFS) and recurrence-free survival (RFS) in basal, luminal A and luminal B breast cancer. Data were collected from GOBO analysis (<http://co.bmc.lu.se/gobo/>). Datasets were stratified into 3 quartiles based on IRG expression (lower, medium and upper quartile) and censored for 10 years follow-up. Logrank P-values are shown as $-\log_{10}(P\text{-value})$.

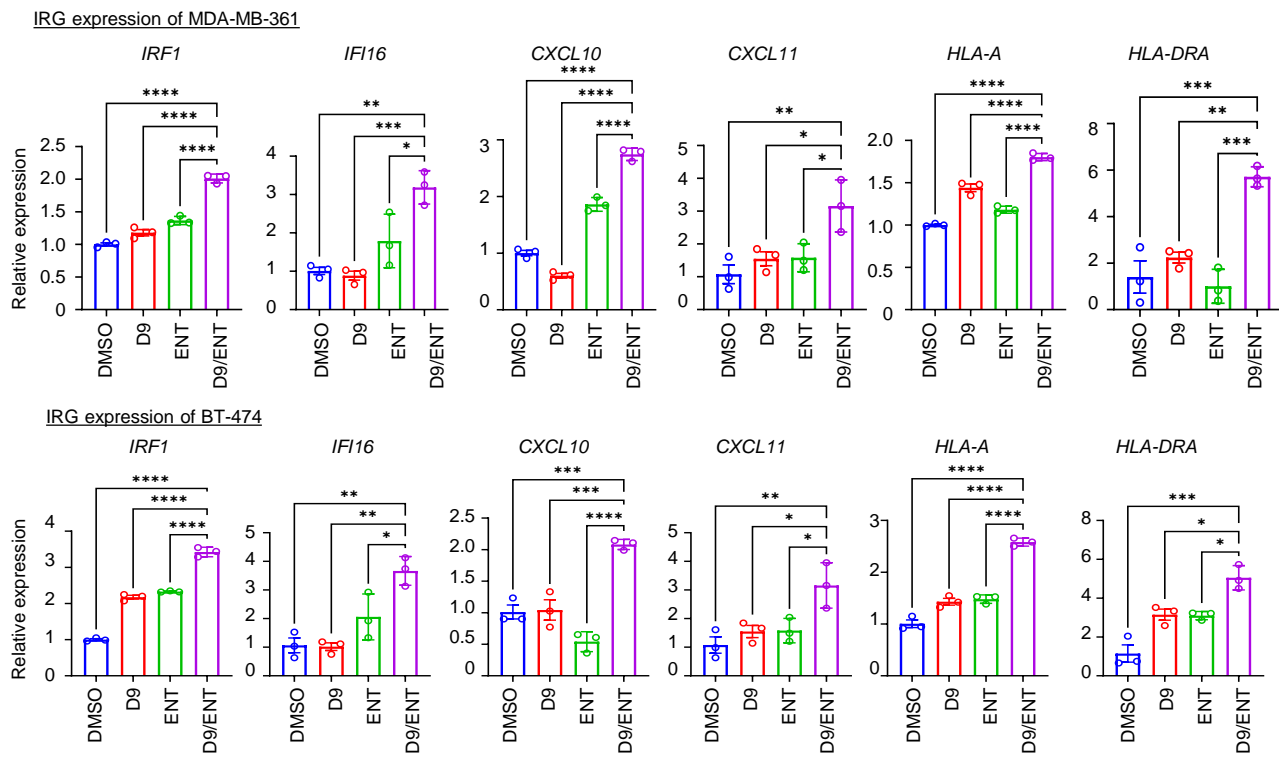
A



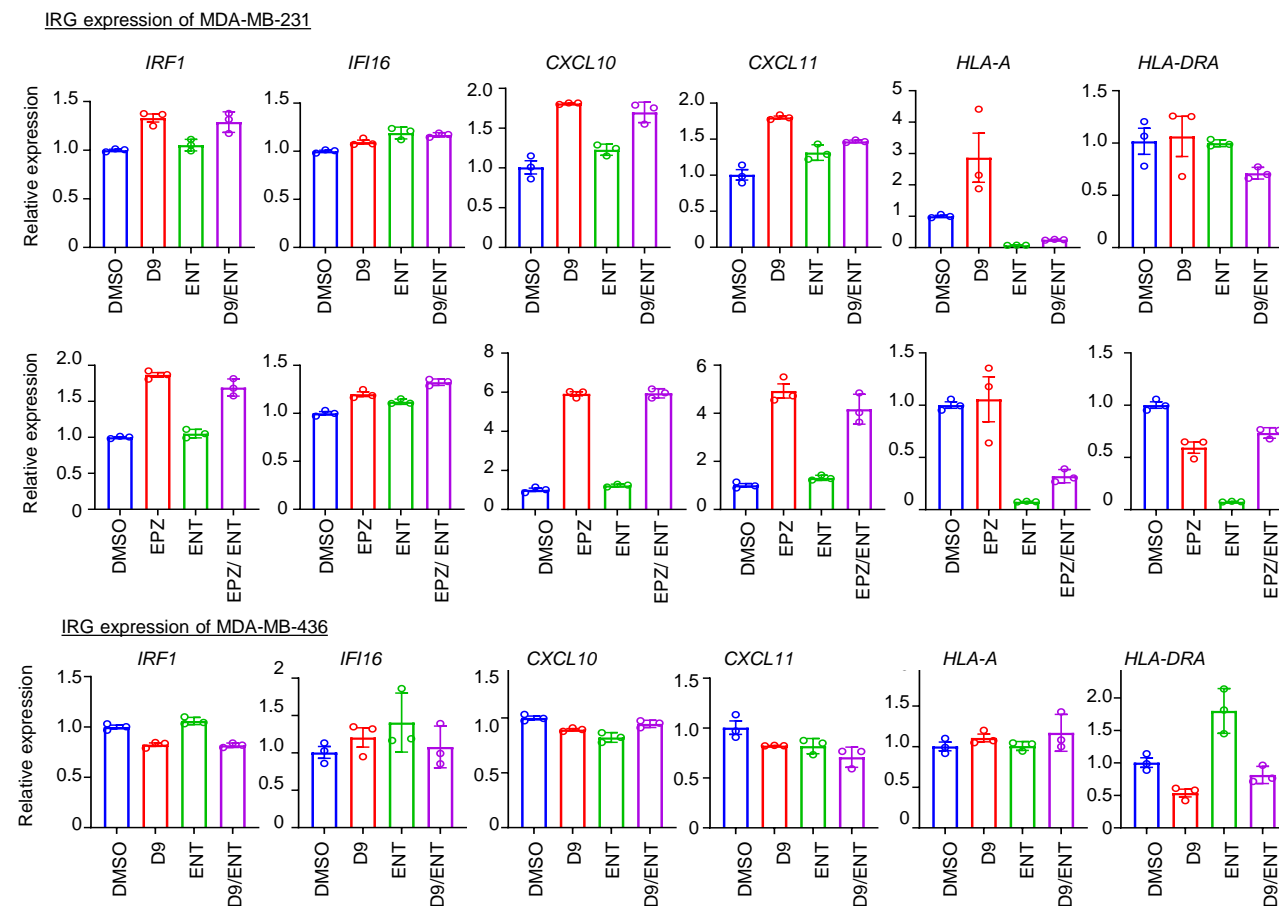
B



C



D



E

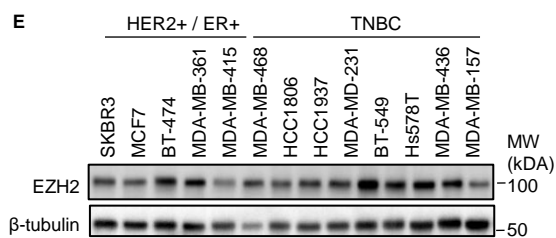
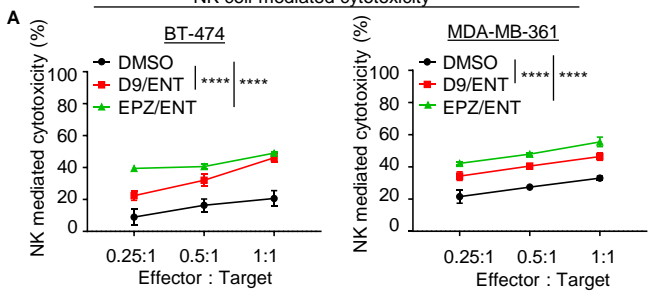
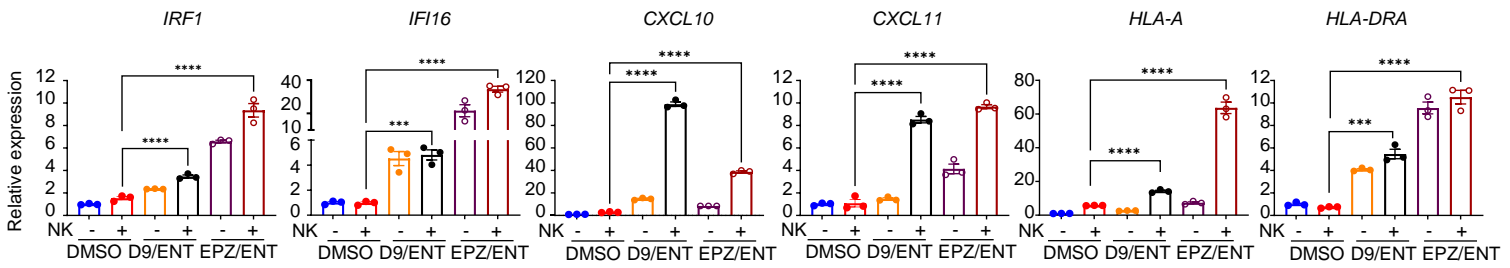


Figure S2: EZH2 and HDAC inhibitors robustly induce IRG expression in HER2+ cells but not in TNBC. (A) RT-PCR analysis showing the expressions of IRG are increased upon EZH2 knockdown in HER2+ SKBR3 cells. Data are expressed as means \pm s.e.m. of three technical replicates, representative of two independent experiments. P value were calculated with one-way ANOVA with Tukey's multiple comparisons test, *P < 0.05, **P < 0.01, ***P < 0.001, ****P < 0.0001, ns not significant. **(B)** Western blot analysis showing the expression of EZH2, H3K27me3 and H3k27ac after single or combinatorial treatment of 250nM ENT and 100nM D9. **(C)** RT-PCR analysis showing epigenetic inhibitors, D9 and ENT induce the expressions of IRG in HER2+ MDA-MB-361 (top) and BT-474 (bottom) cells. **(D)** RT-PCR analysis showing epigenetic inhibitors do not affect the expressions of IRG in TNBC MDA-MB-231 cells (top) and MDA-MB-436 (bottom) cells. Data are expressed as means \pm s.e.m. of three technical replicates, representative of two independent experiments. **(E)** Western blot analysis showing the expression of EZH2 in breast cancer cell lines.

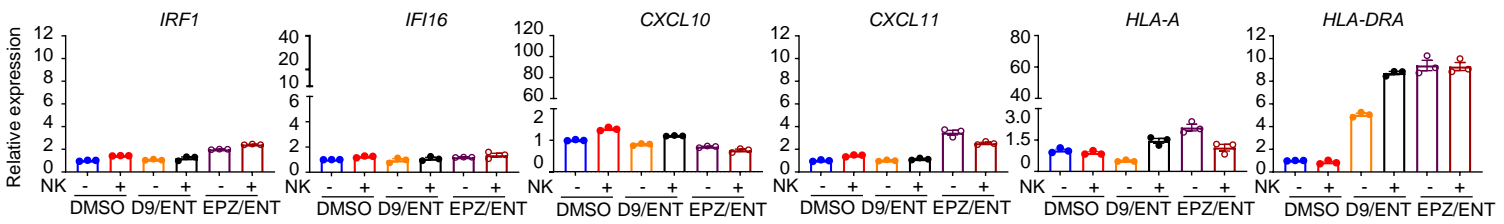
NK cell-mediated cytotoxicity



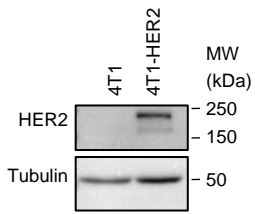
B IRG expression of SKBR3



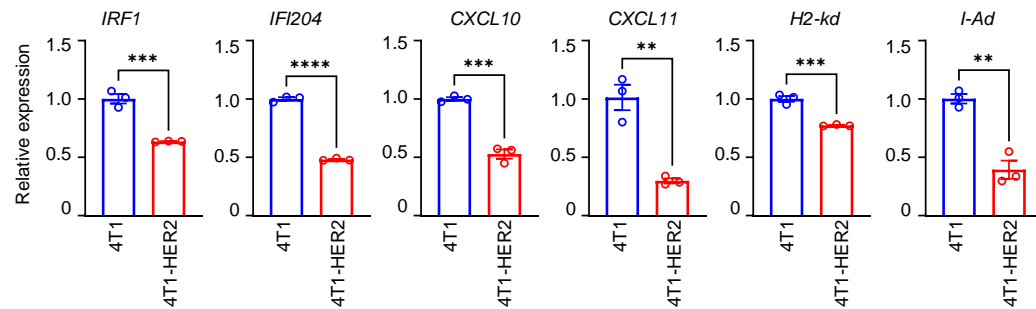
C IRG expression of MDA-MB-231



D



E IRG expression of 4T1 and 4T1-HER2



F IRG expression of 4T1-HER2

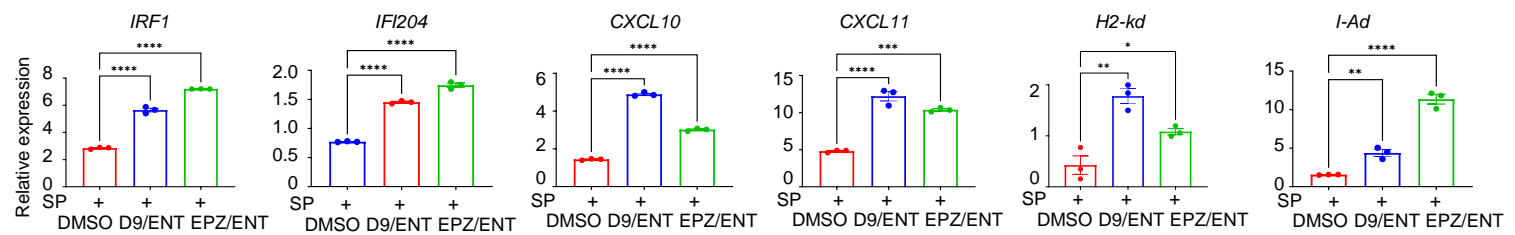


Figure S3: Combinatorial inhibitors of EZH2 and HDAC induce NK cells mediated IRG expression in HER2+ breast cancer. (A)

Representative data showing D9/ENT or EPZ/ENT boosts NK-mediated cytotoxicity of BT-474 and MDA-MB-361 cells. Data are expressed as means \pm s.e.m. of three technical replicates, representative of two independent experiments. P value were calculated with two-way ANOVA with Sidak's multiple comparisons test, *P < 0.05, **P < 0.01, ***P < 0.001, ****P < 0.0001, ns not significant. **(B)** RT-PCR showing the induction of representative IRG in D9/ENT or EPZ/ENT treated SKBR3 and **(C)** MDA-MB-231 cells cocultured with or without NK cells. Data are expressed as means \pm s.e.m. of three technical replicates, representative of two independent experiments. GAPDH was used as a reference gene for normalization. P value were calculated with two-way ANOVA with Sidak's multiple comparisons test, *P < 0.05, **P < 0.01, ***P < 0.001, ****P < 0.0001, ns not significant. **(D)** Western blot showing the overexpression of HER2 in 4T1 mouse mammary cell line to generate 4T1-HER2 cell lines. **(E)** RT-PCR showing the reduction of representative IRG in 4T1-HER2 cells compared to 4T1 cells. Data are expressed as means \pm s.e.m. of three technical replicates, representative of two independent experiments. GAPDH was used as a reference gene for normalization. P value were calculated with unpaired t- test, *P < 0.05, **P < 0.01, ***P < 0.001, ****P < 0.0001, ns not significant. **(F)** RT-PCR showing the induction of representative IRG in D9/ENT or EPZ/ENT treated 4T1-HER2 co-cultured with splenocytes (SP). Data are expressed as means \pm s.e.m. of three technical replicates, representative of two independent experiments. GAPDH was used as a reference gene for normalization. P value were calculated with two-way ANOVA with Sidak's multiple comparisons test. *P < 0.05, **P < 0.01, ***P < 0.001, ****P < 0.0001

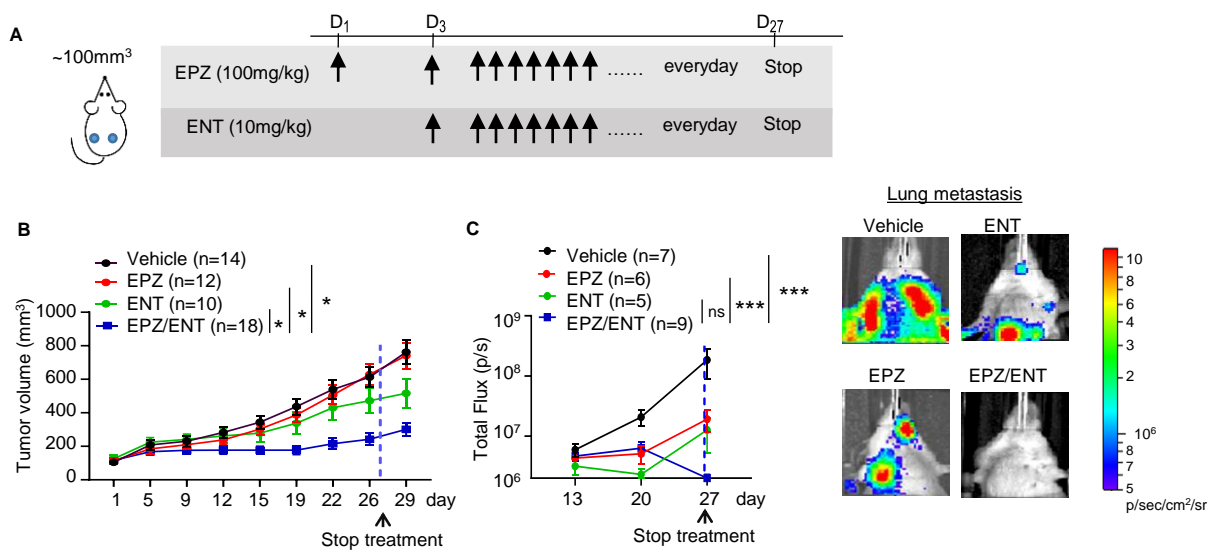
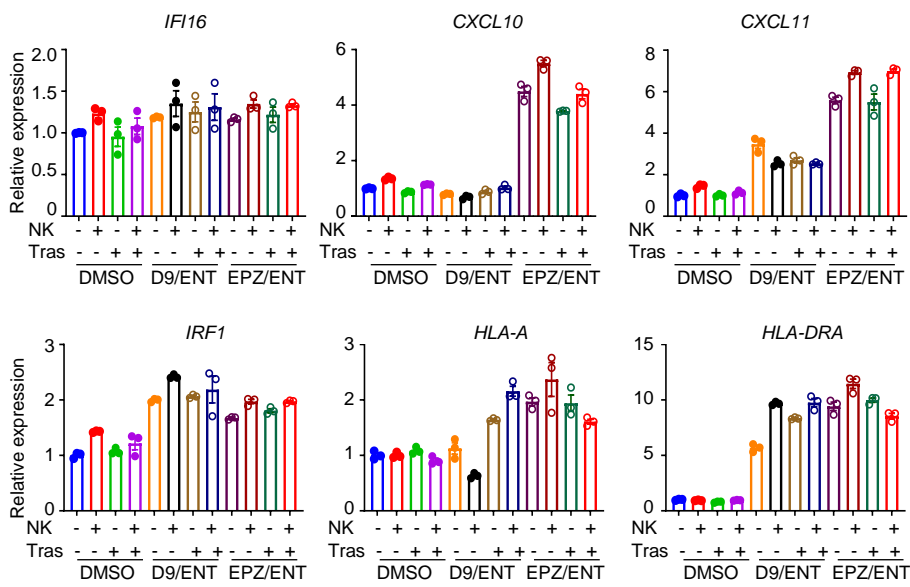


Figure S4: Clinical approved EZH2/HDAC inhibitor suppresses HER2+ tumor growth and metastasis *in vivo*. (A) Illustration of treatment dosage and schedule. Balb/c mice were treated with vehicle, 100 mg/kg EPZ, 10 mg/kg ENT or combination of EPZ/ENT everyday. (B) 4T1-HER2 primary tumor growth of Balb/c mice treated with vehicle, EPZ, ENT or combination of EPZ/ENT. Blue dotted line indicates the day when the treatment was stopped. The number of subjects (n) per group were indicated in the graph. Data are expressed as means \pm s.e.m. of n number of samples. P value were calculated with Mann-Whitney unpaired t-test at endpoints, *P < 0.05, **P < 0.01, ***P < 0.001, ****P < 0.0001, ns not significant. (C) Combination of EPZ/ENT significantly reduced 4T1-HER2 lung metastasis compared to vehicle, EPZ and ENT (left). Representative bioluminescent imaging showing lung metastasis of 4T1-HER2 tumors on day 26 (right). The number of subjects (n) per group were indicated in the graph. Data are expressed as means \pm s.e.m. of n number of samples. P value were calculated with Mann-Whitney unpaired t-test at endpoints, *P < 0.05, **P < 0.01, ***P < 0.001, ****P < 0.0001, ns not significant.

A IRG expression of MDA-MB-231



B

Splenocyte-mediated cytotoxicity

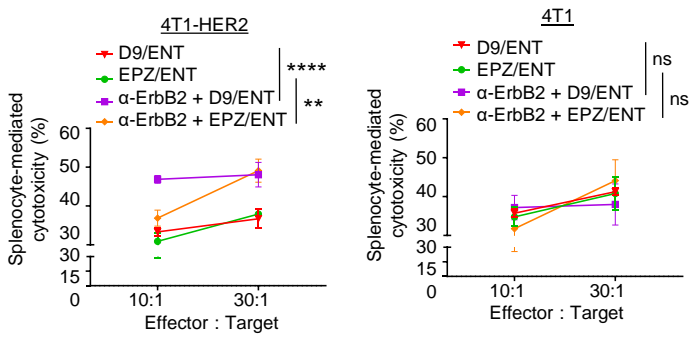


Figure S5: The synergistic effects of epigenetic inhibitors are specific to HER2+ breast cancer. (A) RT-PCR showing the expression of representative IRG in D9/ENT or EPZ/ENT treated MDA-MB-231 cells cocultured with or without NK cells, in the presence of trastuzumab (Tras). Data are expressed as means \pm s.e.m. of three technical replicates, representative of two independent experiments. GAPDH was used as a reference gene for normalization. P values were calculated with one-way ANOVA with Tukey test, *P < 0.05, **P < 0.01, ***P < 0.001, ****P < 0.0001, ns not significant. **(B)** Representative lysis data showing D9/ENT or EPZ/ENT boosts the α -ErbB2 mediated lysis effects, in 4T1-HER2 cells (left) by splenocytes, but not in 4T1 cells (right). Data are expressed as means \pm s.e.m. of three technical replicates, representing two independent experiments. P values were calculated with one-way ANOVA with Tukey's multiple comparison test, *P < 0.05, **P < 0.01, ***P < 0.001, ****P < 0.0001, ns not significant.

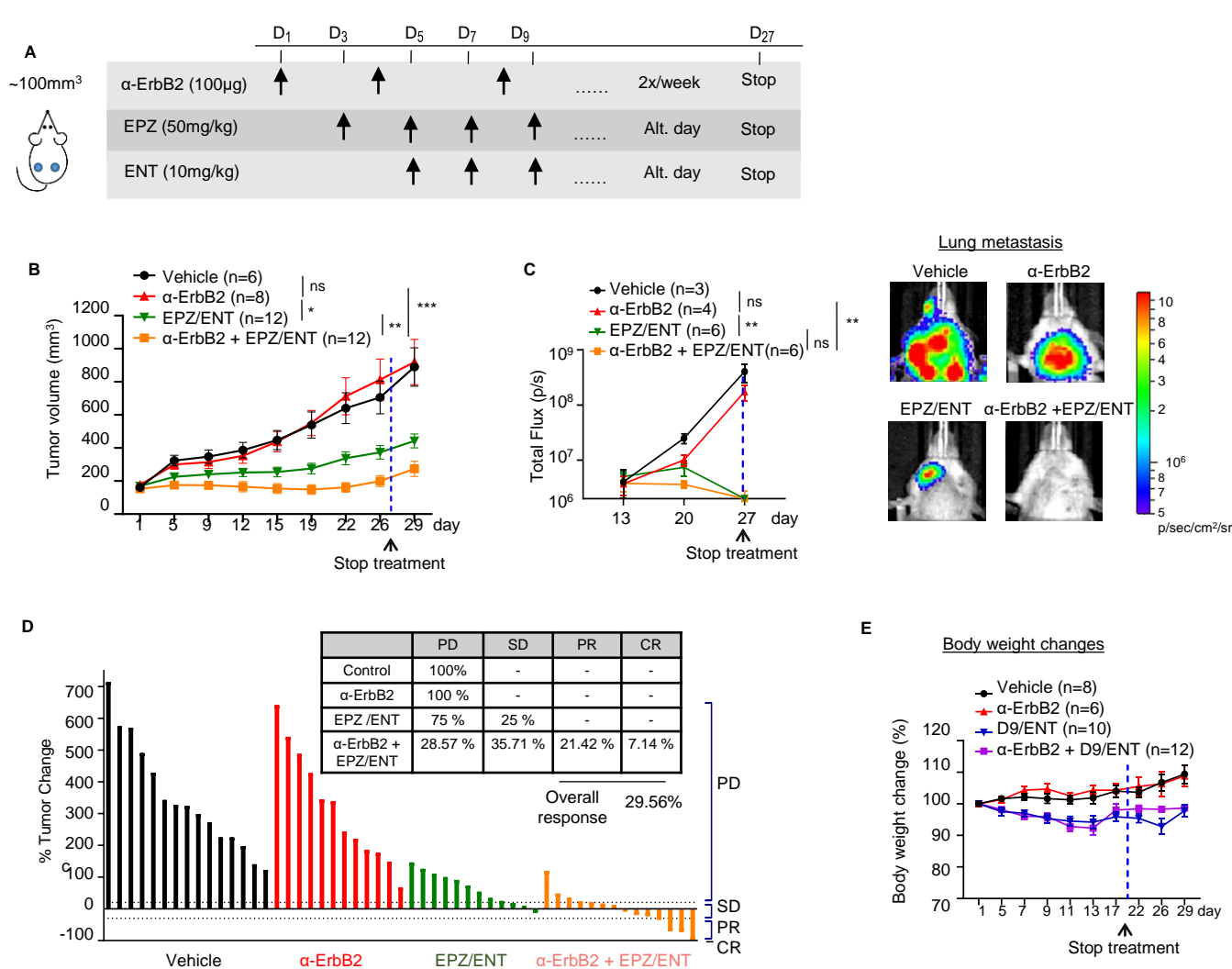


Figure S6: Clinical approved EZH2/HDAC inhibitor sensitized anti-HER2-mediated tumor suppression and metastasis in vivo. (A) Illustration of treatment dosage and schedule. Balb/c mice were treated with vehicle, 100 µg α-ErbB2, 50 mg/kg EPZ and 10 mg/kg ENT, or EPZ/ENT/α-ErbB2. (B) Tumor volume along treatment in 4T1-HER2 tumor bearing Balb/c mice model which were treated with vehicle, α-ErbB2, EPZ and ENT, or EPZ/ENT/α-ErbB2. Blue dotted line indicates the day when the treatment was stopped. The treatment schedule is indicated at the top of the plot. The number of subjects (n) per group were indicated in the graph. Data are expressed as means ± s.e.m. of n number of samples. P value were calculated with Mann-Whitney unpaired t-test based on endpoints, *P < 0.05, **P < 0.01, ***P < 0.001, ****P < 0.0001, ns not significant. (C) α-ErbB2+EPZ/ENT treatment reduces 4T1-HER2 lung metastasis compared to vehicle, α-ErbB2 and D9/ENT treatment (left). Representative bioluminescent imaging showing lung metastasis of 4T1-HER2 tumors on day 26 (right). The number of subjects (n) per group were indicated in the graph. Data are expressed as means ± s.e.m. of n number of samples. P value were calculated with Mann-Whitney unpaired t-test based on endpoints, *P < 0.05, **P < 0.01, ***P < 0.001, ****P < 0.0001, ns not significant. (D) Percentage of tumor change showing the therapeutic effect of α-ErbB2, EPZ/ENT or combination. The percentage of tumor change was calculated based on day 22 from the baseline of tumors before treatment. Tumor volume changes were analyzed based on RECIST criteria to categorize the tumor response into progressive disease (PD), stable disease (SD), progressive repression (PR) and complete response (CR). Each bar represents one individual tumor. (E) Average body weight changes of mice treated with vehicle, 60 mg/kg D9 and 10 mg/kg ENT, 100 µg α-ErbB2, or D9/ENT/α-ErbB2. Blue dotted line indicates the day when the treatment was stopped. The number of subjects (n) per group were indicated in the graph. Data are expressed as means ± s.e.m. of n number of samples.

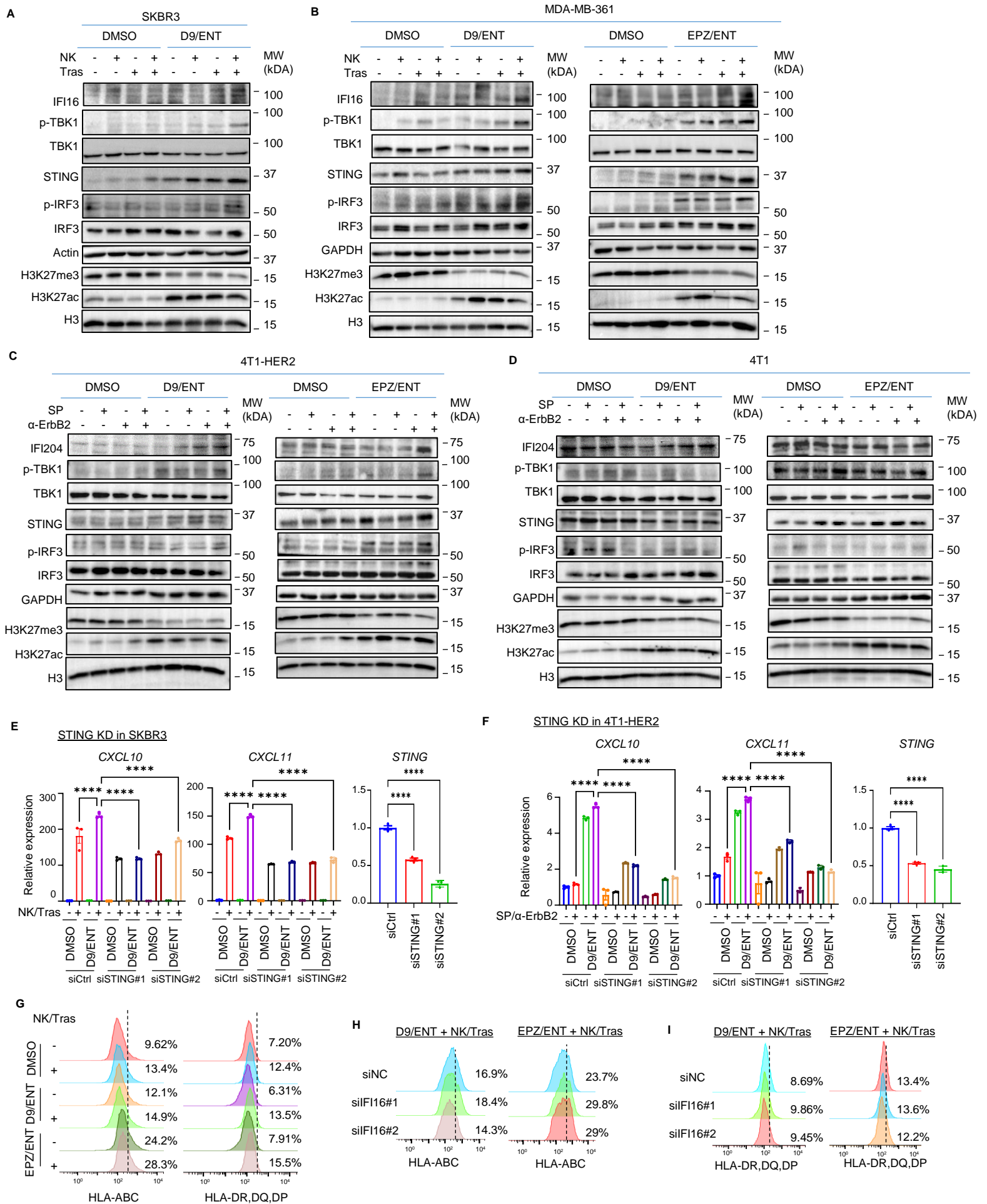


Figure S7: Induction of IFI16-STING pathway by EZH2 and HDAC inhibitor through NK mediated anti-HER2 pathway. (A) Western blot of DMSO or D9/ENT treated SKBR3 and (B) MDA-MB-361 cells cocultured with NK cells and trastuzumab (Tras). Images are representative of two independent experiments. (C) Western blot analysis of DMSO, D9/ENT or EPZ/ENT treated 4T1-HER2 and (D) 4T1 cells cocultured with splenocytes (SP) and α -ErbB2. Images are representative of two independent experiments. (E) Knockdown of STING showing the reduction of CXCL10 and CXCL11 expression in NK/trastuzumab-elicited induction in SKBR3 cells and (F) 4T1-HER2 cells. Data are expressed as means \pm s.e.m. of three technical replicates, representative of two independent experiments. GAPDH was used as a reference gene for normalization. P value were calculated with two-way ANOVA with Sidak's multiple comparisons test for CXCL10 and CXCL11 and one-way ANOVA with Tukey's multiple comparisons test for STING, *P < 0.05, **P < 0.01, ***P < 0.001, ****P < 0.0001, ns not significant. (G) Flow cytometry analysis showing the induction of MHC class I (HLA-ABC) (left) and MHC class II (HLA-DR,DQ, DP) (right) surface expression can be induced by epigenetic inhibitors (D9/ENT or EPZ/ENT) in the presence of NK cells and trastuzumab. Data are representative of two independent experiments. (H) Knockdown of IFI16 does not affect the surface expression of MHC class I (HLA-ABC) and (I) MHC class II (HLA-DR,DQ, DP) induced by epigenetic inhibitors (D9/ENT or EPZ/ENT). Data represent one of two independent experiments.

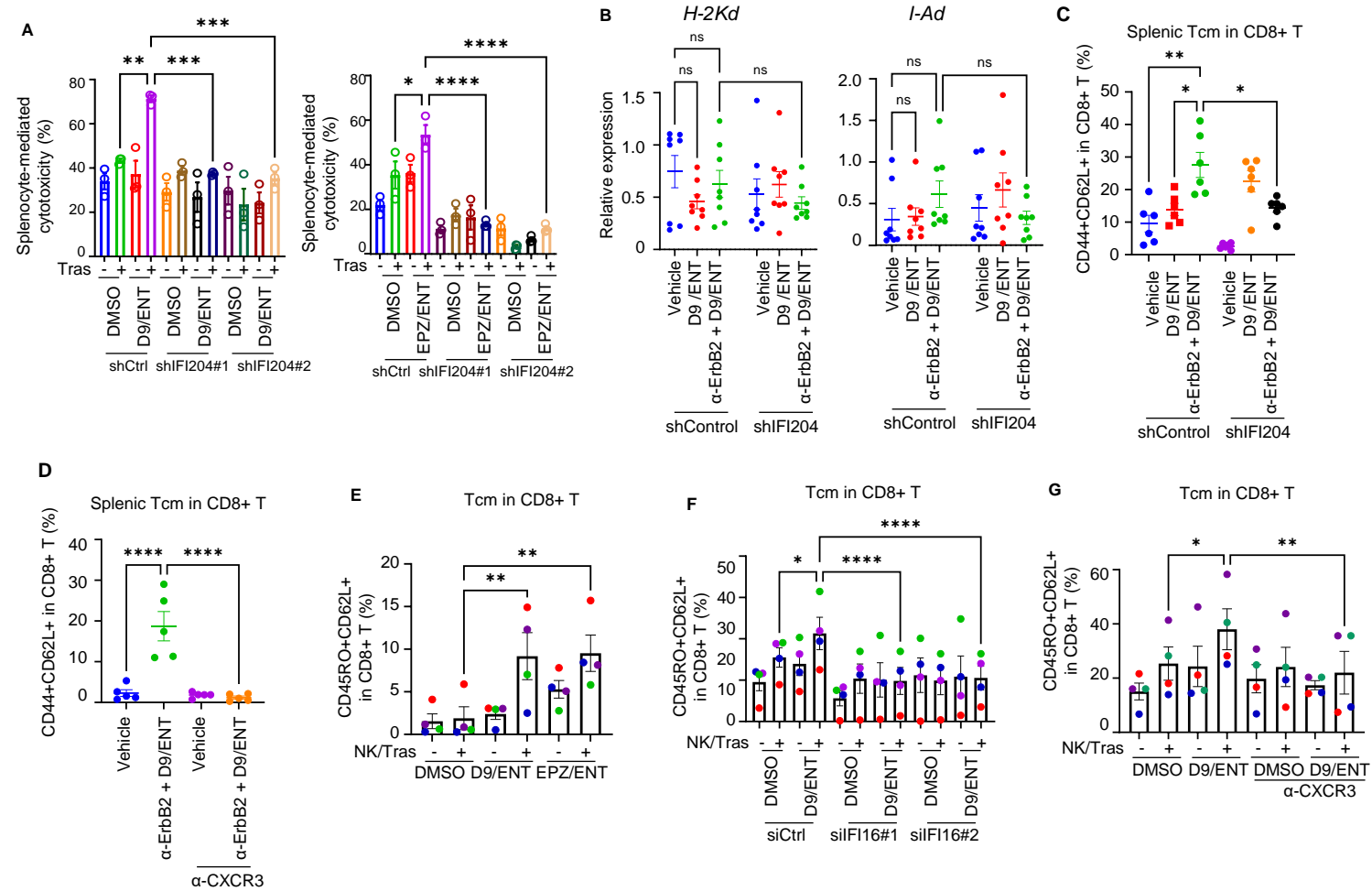


Figure S8: Induction of IFI16-STING pathway by EZH2 and HDAC inhibitor through NK mediated anti-HER2 pathway. (A) Knockdown of IFI204 abolished epigenetic drugs, D9/ENT (left) and EPZ/ENT (right), induced α-ErbB2-mediated cytotoxicity in 4T1-HER2 cells. Data are expressed as means ± s.e.m. of three technical replicates, representative of two independent experiments. P values were calculated with one-way ANOVA with Tukey's multiple comparison test, *P < 0.05, **P < 0.01, ***P < 0.001, ****P < 0.0001, ns not significant. **(B)** RT-PCR showing expression levels of *H2-Kd* and *I-Ad* of 4T1-HER2 tumors. Data are expressed as means ± s.e.m. of eight tumors from each group. P values were calculated two-way ANOVA with Sidak's multiple comparisons test, *P < 0.05, **P < 0.01, ***P < 0.001, ****P < 0.0001, ns not significant. **(C)** Flow cytometry analysis showing the central memory T cells, (Tcm; CD44+CD62L+) population among splenic CD8+ T cells comparing between shControl (shCtrl) and IFI204 knockdown (shIFI204) after corresponding treatment. Spleen were collected at the end of the experiment. Data are expressed as means ± s.e.m. of six spleen samples in each group. P values were calculated with two way ANOVA with Sidak's multiple comparisons test, *P < 0.05, **P < 0.01, ***P < 0.001, ****P < 0.0001, ns not significant. **(D)** Flow cytometry analysis showing the central memory T cells (Tcm; CD44+CD62L+) population among splenic CD8+ T cells with or without the addition of CXCR3 inhibitor upon corresponding treatment. Spleen were collected at the end of the experiment. Data are expressed as means ± s.e.m. of five spleen samples in each group. P values were calculated with two way ANOVA with Sidak's multiple comparisons test, *P < 0.05, **P < 0.01, ***P < 0.001, ****P < 0.0001, ns not significant. **(E)** Flow cytometry analysis showing coculture of CD8+ T cells with D9/ENT and EPZ/ENT treated SKBR3 in the presence of NK cells and trastuzumab could induce the formation of central memory T cells (Tcm; CD45RO+CD62L+ population). Data are expressed as means ± s.e.m. of four individual donors. Each colour dot represents an individual donor. P values were calculated two-way ANOVA with Sidak's multiple comparisons test, *P < 0.05, **P < 0.01, ***P < 0.001, ****P < 0.0001, ns not significant. **(F)** Knockdown of IFI16 and **(G)** blockade of CXCR3 diminished the induction of CD8+ central memory T cells induced by D9/ENT and EPZ/ENT treated SKBR3 in the presence of NK cells and trastuzumab. Data are expressed as means ± s.e.m. of four individual donors. Each colour dot represents an individual donor. P values were calculated two-way ANOVA with Sidak's multiple comparisons test, *P < 0.05, **P < 0.01, ***P < 0.001, ****P < 0.0001, ns not significant.

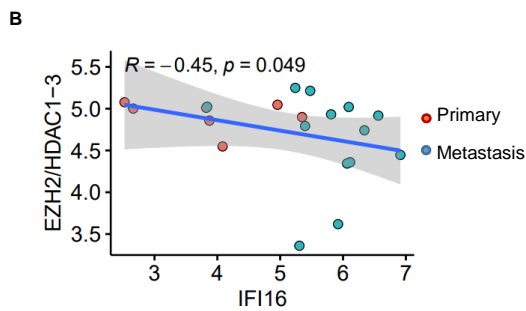
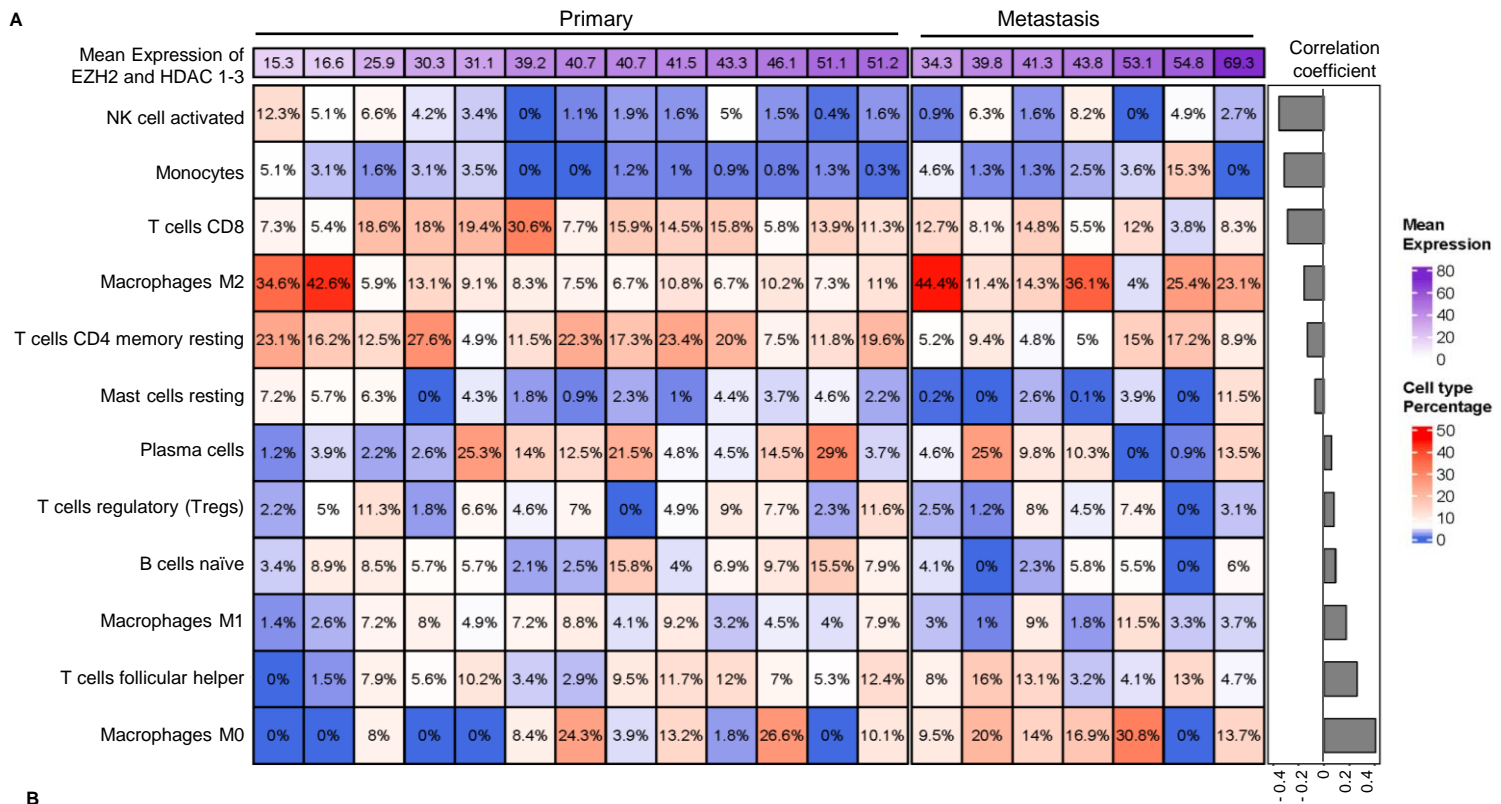
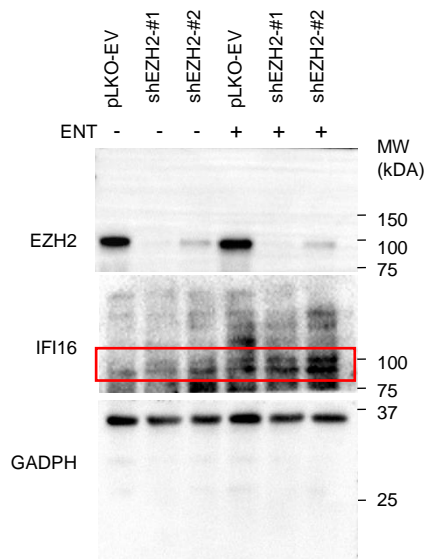
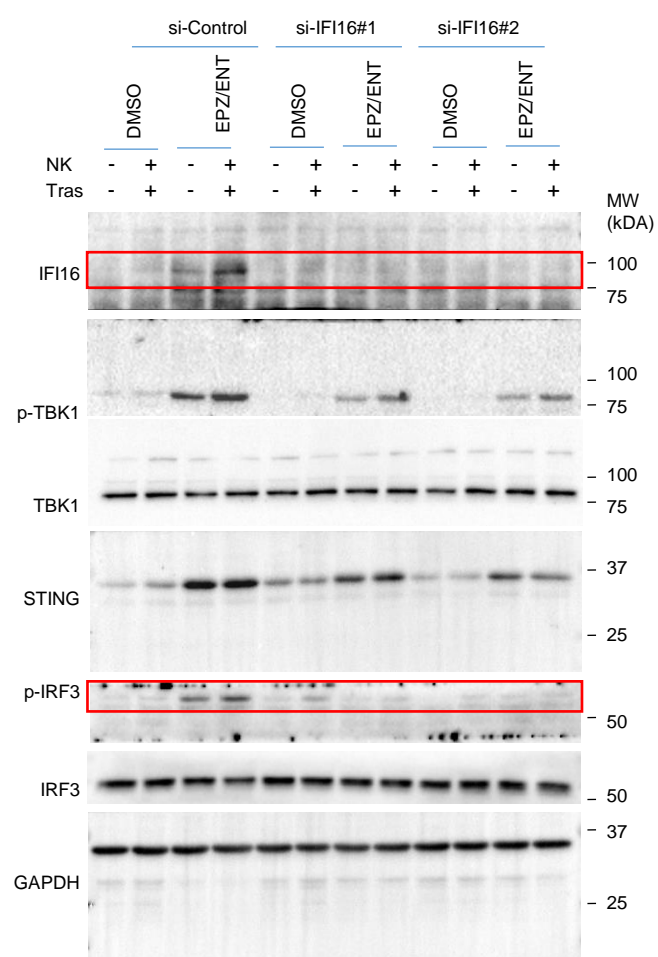


Figure S9: Correlation of EZH2/HDAC 1 – 3 expression with tumor infiltrating immune cells and IFI16 expression. (A) Heatmap showing correlation of EZH2/HDAC 1-3 and tumor infiltrating immune cells in primary and metastatic HER2+ tumors (n=20) deconvoluted using Cibersortx (<https://cibersortx.stanford.edu/>). Immune cell type absent (cell fraction percentage = 0%) in more than 75% of tumors were removed from the correlation analysis. **(B)** Correlation between EZH2/HDAC1-3 and IFI16 expression in primary and metastatic HER2+ tumor. Each dot represents one patient (n=20). The linear regression Spearman's correlation coefficient (R) and P values are calculated.

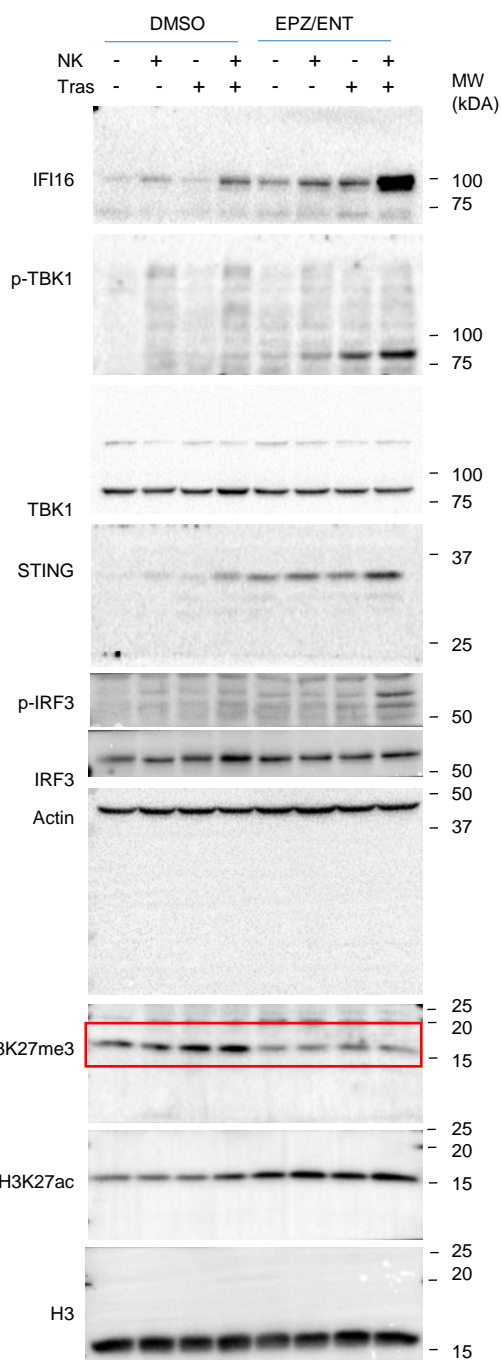
Uncropped Western blot for Figure 7F



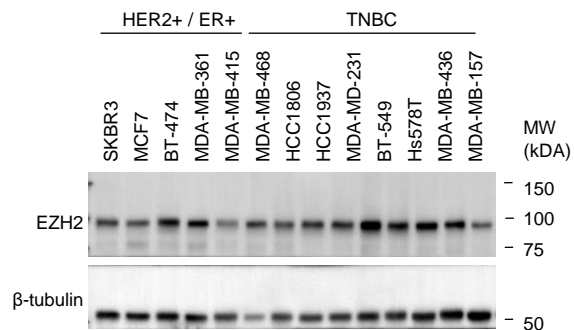
Uncropped Western blot for Figure 7H



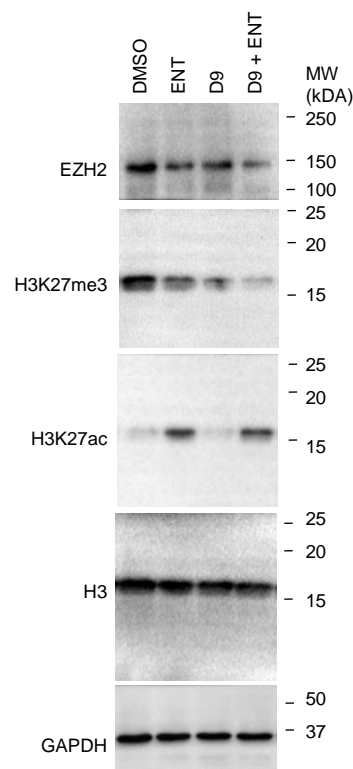
Uncropped Western blot for Figure 7G



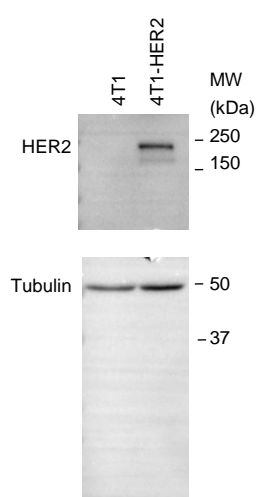
Uncropped Western blot for Supplementary figure 2A



Uncropped Western blot for Supplementary figure 2C



Uncropped Western blot for Supplementary figure 3D



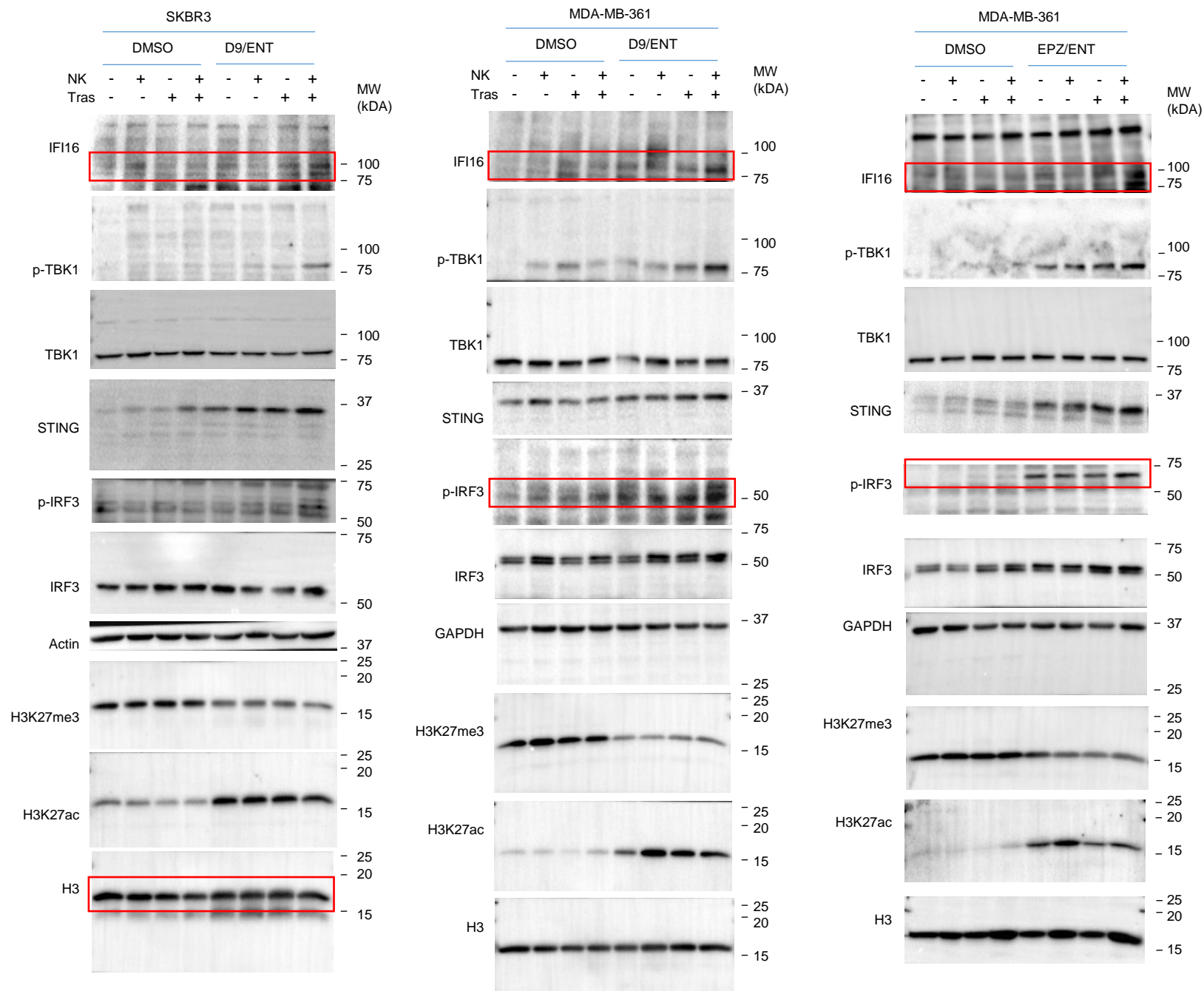


Figure S11 Uncropped western blots

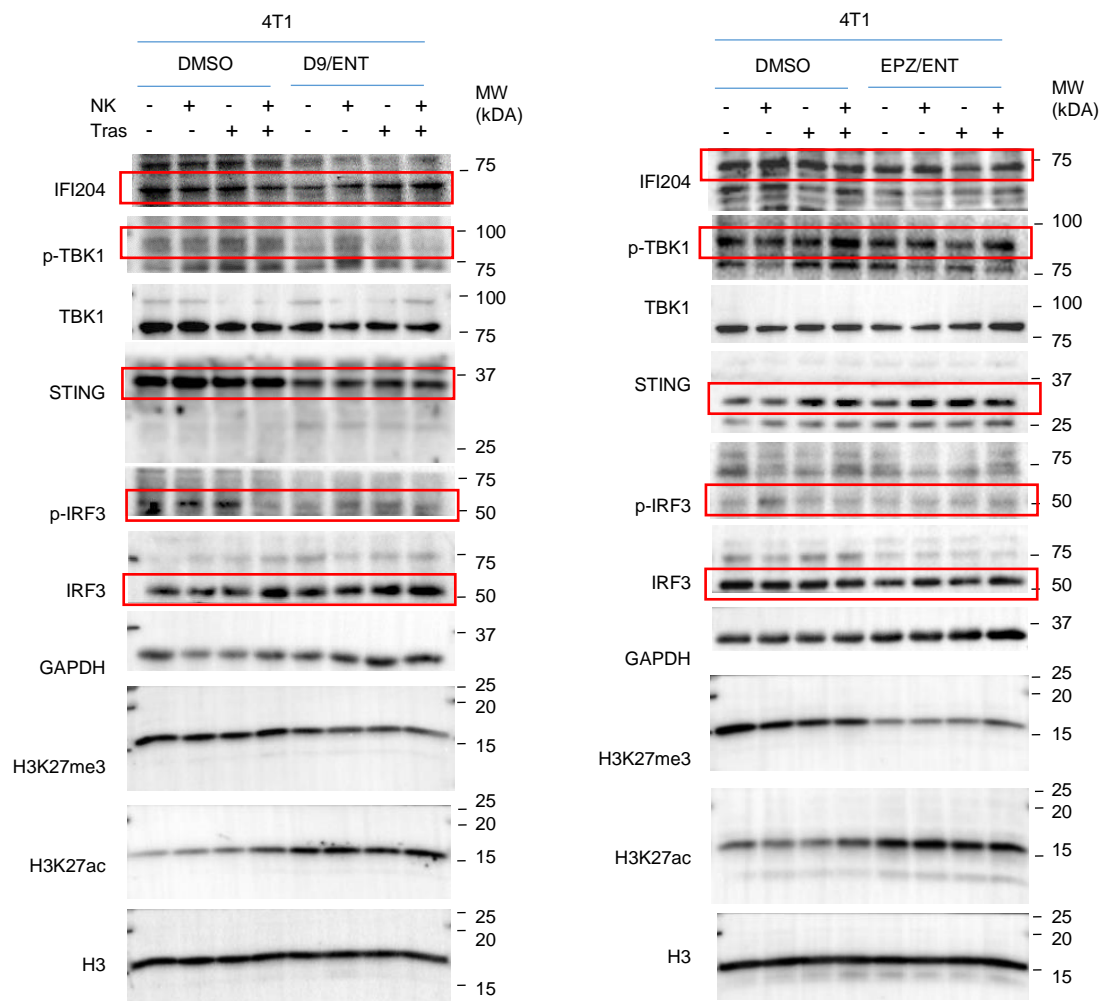
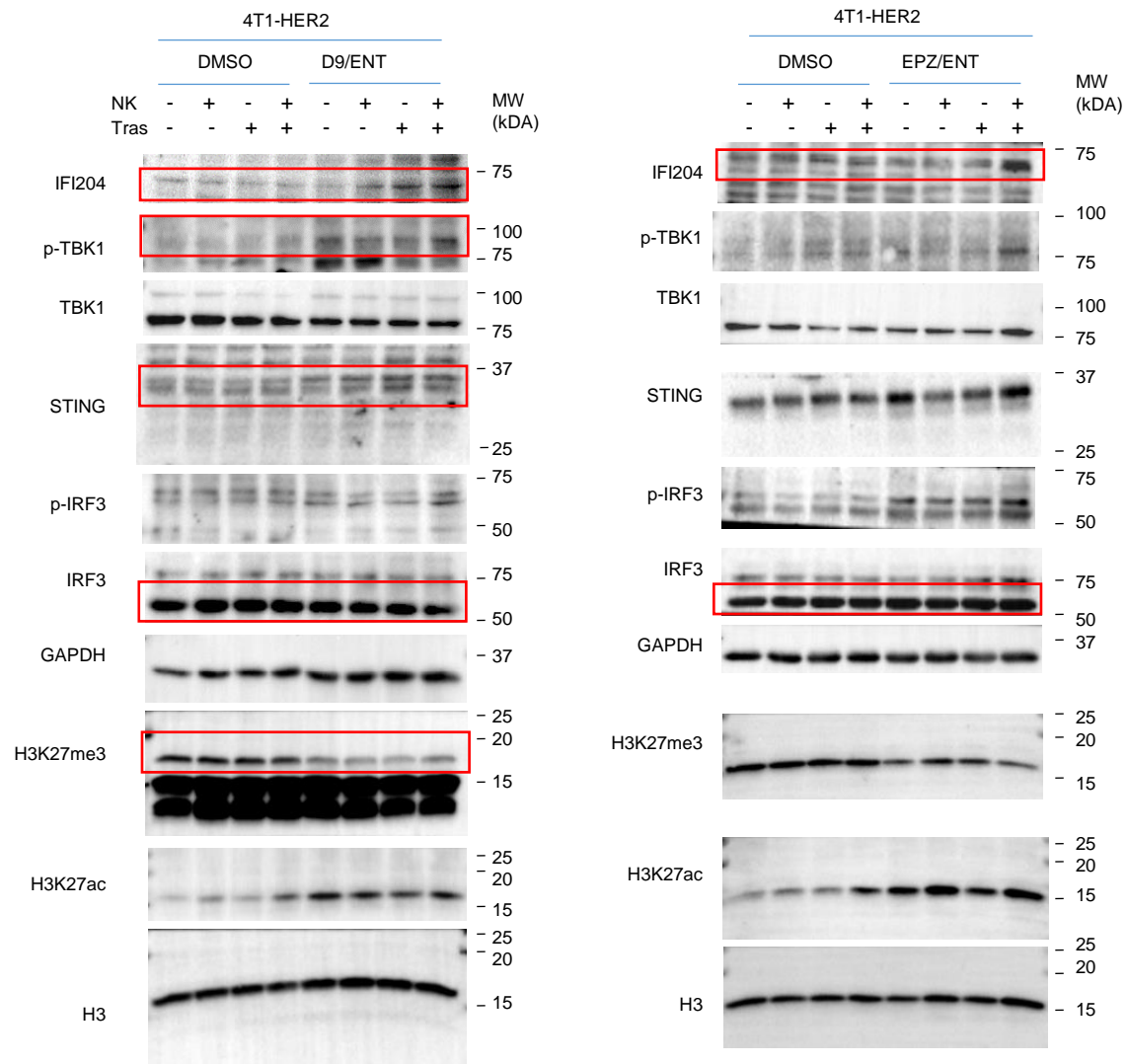


Table S1: Averaged fold-change induction of 6 representative IRG derived from microarray analysis different breast cancer subtypes treated with various combinations of various epigenetic inhibitors.

| | SKBR3 | | | | | | | MDA-MB-231 | | | | MCF10A | | | |
|----------------|---------|--------|--------|-------|----------------|--------------|----------------|------------|-------|-------|----------------|---------|-------|-------|----------------|
| | Control | DZNep | TSA | AZA | DZNep + AZA | AZA + TSA | DZNep + TSA | Control | DZNep | TSA | DZNep + TSA | Control | DZNep | TSA | DZNep + TSA |
| <i>IFI16</i> | 1.000 | 0.220 | 1.669 | 1.373 | 0.432 | 0.593 | 27.432 | 1.000 | 0.769 | 0.897 | 0.491 | 1.000 | 0.711 | 0.902 | 0.418 |
| <i>IRF1</i> | 1.000 | 2.717 | 1.454 | 1.185 | 3.089 | 1.546 | 4.746 | 1.000 | 2.959 | 1.139 | 4.182 | 1.000 | 1.257 | 1.090 | 2.085 |
| <i>CXCL10</i> | 1.000 | 10.751 | 1.331 | 0.847 | 8.810 | 1.584 | 100.252 | 1.000 | 4.264 | 1.701 | 2.806 | 1.000 | 0.510 | 0.371 | 0.645 |
| <i>CXCL11</i> | 1.000 | 3.105 | 2.407 | 2.185 | 7.852 | 2.179 | 33.599 | 1.000 | 5.333 | 2.800 | 5.017 | 1.000 | 0.818 | 0.323 | 0.606 |
| <i>HLA-A</i> | 1.000 | 1.641 | 1.370 | 1.389 | 2.686 | 2.212 | 3.591 | 1.000 | 0.957 | 1.203 | 1.044 | 1.000 | 0.827 | 0.979 | 1.143 |
| <i>HLA-DRA</i> | 1.000 | -0.407 | -1.441 | 1.441 | 1.424 | 2.508 | 36.949 | 1.000 | 0.726 | 1.238 | 0.769 | 1.000 | 0.900 | 1.100 | 0.020 |

Table S2: Primers for qRT-qPCR

| Species | Genes | Forward primer (5' → 3') | Reverse primers (5' → 3') |
|----------------|----------------|---------------------------------|----------------------------------|
| Human | <i>IRF1</i> | GAGGAGGTGAAAGACCAGAGCA | TAGCATCTCGGCTGGACTTCGA |
| | <i>IFI16</i> | ACTGAGTACAACAAAGCCATTTGA | TTGTGACATTGTCCTGTCCCCAC |
| | <i>CXCL10</i> | TCCACGTGTTGAGATCATTGCT | TCTTGATGGCCTTCGATTCTGG |
| | <i>CXCL11</i> | AGTTGTTCAAGGCTTCCCCA | TCTGCCACTTTCACTGCTTT |
| | <i>HLA-A</i> | GGACCAGGAGACACGGAATG | GGATGGTGTGAGAACCGGC |
| | <i>HLA-DRA</i> | CCGATCACCAATGTACCTCC | CACTGGTGGGGTGAACCTTGT |
| | <i>CITTA</i> | CTACTTCAGGCAGCAGAGGAGA | GCTGTGTCTTCCGAGGAACTTC |
| | <i>EZH2</i> | AGTGTGACCCTGACCTCTGT | AGATGGTGCCAGCAATAGAT |
| | <i>HER2</i> | CGCAGCTCATCTACCAGGAG | AAATACATCGGAGCCAGCCC |
| | <i>GAPDH</i> | CACCATCTTCCAGGAGCGAG | AAATGAGCCCCAGCCTTCTC |
| Mouse | <i>IRF1</i> | GGCCGATACAAAGCAGGAGAA | GGAGTTCATGGCACAACGGA |
| | <i>IFI204</i> | ATGTCAGGTGTGAACCAGGC | CCTTACAGACCTCAGCTGCC |
| | <i>CXCL10</i> | CCAAGTGCTGCCGTCATTTTC | TCCCTATGGCCCTCATTCTCA |
| | <i>CXCL11</i> | CCGAGTAACGGCTGCGACAAAG | CCTGCATTATGAGGCGAGCTTG |
| | <i>H2-Kd</i> | GAGGAGCAGACACAGAGAGC | GAACATCCGCTGGAACGTGT |
| | <i>I-Ad</i> | AGAGCTCTGATTCTGGGGGT | ATAGAAGCCTACGTGGTCGG |
| | <i>GAPDH</i> | CATCACTGCCACCCAGAAGACTG | ATGCCAGTGAGCTTCCCGTTCAG |

Table S3: Target sequences of shRNA transfection

| shRNA | Sequences (5' → 3') |
|--------------|----------------------------|
| shEZH2#1 | GGTGAATGCCCTTGGTCAATA |
| shEZH2#2 | GCAAAGCTTACACTCCTTTC |
| shIFI204#1 | CTGAAAACAATTGACAGGCAAC |
| shIFI204#2 | CGGAGAGGAATAAATTCATTTA |

Table S4: Target sequences of siRNA transfection

| DsiRNA | Duplex sequence (5' → 3') | Duplex sequence (5' → 3') |
|---------------|----------------------------------|----------------------------------|
| siF116#1 | UGGAUGUCAUUGACGAUAAUGUUTA | UAAACAUUAUCGUCAAUGACAUCCAGA |
| siF116#2 | GAAACUCUGAAGAUUGAUUUCUTC | GAAGAAUAUCAAUUCUUCAGAGUUUCCU |

Table S5: Primers for RT-qPCR for ChIP samples

| Genes | ChIP forward primer (5' → 3') | ChIP reverse primers (5' → 3') |
|--------------|--------------------------------------|---------------------------------------|
| IFI16-1 | CTGGGGTTACAGCACGCTAA | TCCGGTAGTGTGAGGAGTCT |
| IFI16-2 | GGGTGCTAGCGGCAGAATTT | TAACTGCCTTCCCCTCCACT |
| Actin | CCGAAAGTTGCCTTTTATGG | CAAAGGCGAGGCTCTGTG |

SI References

1. S. A (2010) FASTQC. A quality control tool for high throughput sequence data.
2. Ewels P. MM, Lundin S., Käller M. (2016) MultiQC: summarize analysis results for multiple tools and samples in a single report. *Bioinformatics* 31:3047–3048.
3. Kim D, Langmead, B., Salzberg, S.L. (2015) HISAT: a fast spliced aligner with low memory requirements. *Nat. Methods* 12:357–360.
4. Liao Y SG, Shi W. (2014) featureCounts: an efficient general purpose program for assigning sequence reads to genomic features. *Bioinforma. Oxf. Engl.* 30:923-930 <https://doi.org/910.1093/bioinformatics/btt1656>.
5. Wang L. WS, Li W. (2012) RSeQC: quality control of RNA-seq experiments. *Bioinforma. Oxf. Engl.* 28:2184–2185 <https://doi.org/2110.1093/bioinformatics/bts2356>.
6. McCarthy DJ CY, Smyth GK. (2012) Differential expression analysis of multifactor RNA-Seq experiments with respect to biological variation. *Nucleic Acids Res.* 40:4288–4297. <https://doi.org/4210.1093/nar/gks4042>.
7. Robinson MD MD, Smyth GK. (2010) edgeR: a Bioconductor package for differential expression analysis of digital gene expression data. *Bioinformatics* 26:139–140.
8. Rusinova I FS, Yu S, Kannan A, Masse M, Cumming H, Chapman R, Hertzog PJ.(2013) INTERFEROME v2.0: an updated database of annotated interferon-regulated genes. *Nucleic Acids Res.* 41:D1040–D1046. <https://doi.org/1010.1093/nar/gks1215>.
9. Subramanian A TP, Mootha VK, Mukherjee S, Ebert BL, Gillette MA, Paulovich A, Pomeroy SL, Golub TR, Lander ES, Mesirov JP. (2005) Gene set enrichment analysis: A knowledge-based approach for interpreting genome-wide expression profiles. *Proc. Natl. Acad. Sci.* P102:15545–15550.
10. Liberzon A. BC, Thorvaldsdóttir H., Ghandi M., Mesirov JP, Tamayo P. (2015) The Molecular Signatures Database (MSigDB) hallmark gene set collection. *Cell Syst.* 1:417–425. <https://doi.org/410.1016/j.cels.2015.1012.1004>.
11. Yu G WL-G, Han Y, He Q-Y (2012) clusterProfiler: an R package for comparing biological themes among gene clusters. *OMICS J. Integr. Biol.* 16:284–287. <https://doi.org/210.1089/omi.2011.0118>.
12. Nirmal AJ RT, Shih BB, Hume DA, Sims AH, Freeman TC (2018) Immune cell gene signatures for profiling the microenvironment of solid tumors. *Cancer Immunology Research* 6(11):1388-1400.
13. Steen CB LC, Alizadeh AA, Newman AM (2020) Profiling Cell Type Abundance and Expression in Bulk Tissues with CIBERSORTx. *Methods Mol. Biol.* 2117:135-157.
14. Langmead B, Salzberg, S.L. (2012) Fast gapped-read alignment with Bowtie 2. *Nat. Methods* 9:357–359. <https://doi.org/310.1038/nmeth.1923>.
15. Li H HB, Wysoker A, Fennell T, Ruan J, Homer N, Marth G, Abecasis G, Durbin R (2009) The Sequence Alignment/Map format and SAMtools. *Bioinformatics* 25:2078–2079. <https://doi.org/2010.1093/bioinformatics/btp2352>.
16. Ramírez F RD, Grüning B, Bhardwaj V, Kilpert F, Richter AS, Heyne S, Dündar F, Manke T. (2016) deepTools2: a next generation web server for deep-sequencing data analysis. *Nucleic Acids Res.* 44:W160-165. <https://doi.org/110.1093/nar/gkw1257>.
17. Zhang Y LT, Meyer CA, Eeckhoutte J, Johnson DS, Bernstein BE, Nusbaum C, Myers RM, Brown M, Li W, Liu XS. (2008) Model-based Analysis of ChIP-Seq (MACS). *Genome Biol.* 9:R137. <https://doi.org/110.1186/gb-2008-1189-1189-r1137>.
18. Yu G WL-G, Han Y, He Q-Y (2015) ChIPseeker: an R/Bioconductor package for ChIP peak annotation, comparison and visualization. *Bioinforma. Oxf. Engl.* 31:2382–2383. <https://doi.org/2310.1093/bioinformatics/btv2145>.